# Wave Equation Migration with Attenuation Compensation

*A.A. Valenciano, N. Chemingui,* D. Whitmore and S. Brandsberg-Dahl (PGS)*



## Abstract

We introduce a new viscoacoustic Wave Equation Migration (WEM) for media with attenuation. Our solution is based on a Fourier Finite-Difference (FFD) scheme for migration by wavefield continuation. Similarly to the acoustic solution, the viscoacoustic migration consists of three terms: a phase-shift extrapolation, a thin-lens correction, and a finite-differences operation. The dispersion relation, in presence of attenuation, includes both real and imaginary terms. While the real part controls the kinematics of the image, the imaginary part recovers the high wavenumber components in the seismic image; therefore improving resolution and amplitude balance. The viscoacoustic migration is also extended to account for anisotropy (VTI and TTI). The anisotropic effects are incorporated in the migration by using odd and even rational function terms in the finite differences solution. The implementation is stable, efficient, and very flexible. In absence of attenuation or anisotropy, the solution reduces to the familiar isotropic acoustic case. Results from synthetic example and two dual sensor field surveys from the North Sea and the Gulf of Mexico demonstrate the importance of incorporating the attenuation effects in the migration algorithm.

## Introduction

Attenuation of seismic waves by the earth causes a loss of high-frequency energy, and a general distortion of the wavelet's phase. Seismic attenuation and dispersion are usually compensated for in the time domain during data conditioning and preprocessing. These compensation techniques are typically one-dimensional, strictly valid if the earth attenuation, described by the quality factor (Q), is constant. When the Q model varies laterally, the 1D compensation is not accurate, especially in complex geology that causes complicated ray paths e.g., shallow hydrates in the Gulf of Mexico, shallow gas clouds in the North Sea, etc…(Chen and Huang, 2010; Yu et al., 2002). Incorporating the Q compensation into a viscoacoustic wave-equation prestack depth migration (PSDM) is therefore a better alternative since the migration can handle the ray path complexity.

Q compensation in a viscoacoustic PSDM has been implemented in the context of one-way wave-equation migration (WEM) by: Dai and West (1994) using phase-shift methods, Mittet et al. (1995) using explicit finite-differences, Yu et al. (2002) using PSPI, and Wang (2008) using implicit finite differences. It has been also implemented in reverse time migration by Causse and Ursin (2000), and Zhang et al. (2010). With adequate estimation of a Q model, these migrations potentially produce images with correct depth positioning and amplitude information, within the limitations of the algorithm, including an isotropic velocity.

In this paper we present a one-way wave equation approach that allows us to accurately image data in anisotropic media with attenuation. This is achieved through an extension of the Fourier Finite-Differences (FFD) algorithm (Ristow and Ruhl, 1994) to compensate for the effects of Q during migration. This mixed-domain one-wave wave-equation algorithm is flexible and efficient, in addition to its accuracy for imaging complex geology particularly below salt. Previously, Valenciano et al. (2009) extended the algorithm to account for tilted transverse anisotropy (TTI). In this work we show that the method can be further extended to include attenuation compensation. Consequently, the attenuation and the anisotropy of the medium can be properly handled by one FFD viscoacoustic PSDM solution. We demonstrate using a synthetic, and two field data examples that the effects of attenuation can be mitigated by the proposed FFD viscoacoustic WEM.

## Method

In a linear attenuating medium the constant-density viscoacoustic wave-equation can be expressed as

$$\left[\frac{\omega^2}{V^2(\omega,x,y,z)}+\Delta\right]P(\omega,x,y,z)=0, \qquad (1)$$

where $P$ is the pressure, $\omega$ is the angular frequency, $V$ is the frequency-dependent velocity, and $\Delta$ is the 3D Laplacian. In a homogeneous medium, equation (1) has the following phase-shift recursive solution:

$$P(z+\Delta z;\omega,k_x,k_y)=P(z;\omega,k_x,k_y)\exp(\pm ik_z\cdot\Delta z) \qquad (2)$$

where $k_z$ is the vertical wavenumber, and $k_x$ and $k_y$ are the horizontal wavenumbers. The plus and minus signs in the phase shift operator represent downgoing and upgoing waves, respectively.

The dispersion relation, as function of normalized wavenumbers, is given by:

$$s_{zQ}=\sqrt{\left(1+\frac{i}{2Q}\right)^2-s_x^2-s_y^2} \qquad where$$
$$s_{zQ}=\frac{v(\omega)}{\omega}k_{zQ}\,,\;\; s_x=\frac{v(\omega)}{\omega}k_x \;\; and \;\; s_y=\frac{v(\omega)}{\omega}k_y \qquad (3)$$

Generally, both the quality factor *Q* and the phase velocity *v* are frequency dependent. Several models have been proposed to fit the dependence of Q on frequency using laboratory and field observations. In our inverse-Q wave equation PSDM method, we use the nearly constant Q model originally proposed by Futterman (1962) and then adapted by Robinson (1979), where the phase velocity is expressed as:

$$v(\omega) = v(\omega_r)\left[1 - \frac{1}{\pi Q(\omega_r)}\ln(\omega/\omega_r)\right]^{-1}, \qquad (4)$$

with $Q(\omega_r)$ and $v(\omega_r)$ being the quality factor and phase velocity at a reference frequency $\omega_r$. We assume that frequency dependence of *Q* is not significant over the seismic frequency range and therefore we consider it to be constant with frequency.

**The Fourier Finite Differences (FFD) solution**

The phase-shift migration operator described above is strictly valid for a subsurface model that varies only with depth. To extend the operator to handle laterally varying earth models, we take a similar approach to that for deriving the acoustic FFD migration (Ristow and Ruhl, 1994). For simplicity we illustrate the derivations of the FFD approximation in 2D whereas the algorithm was implemented fully in 3D.

Starting from the difference between the operator $k_{zQ}$ (dispersion relation) in the inhomogeneous medium, and that in the background medium

$$D = \frac{\omega}{v(\omega)}\sqrt{\left(1+\frac{i}{2Q}\right)^2 - s_x^2} - \frac{\omega}{v_0(\omega)}\sqrt{\left(1+\frac{i}{2Q_0}\right)^2 - s_{x0}^2} \qquad (5)$$

we can rewrite the difference from equation 5 as

$$D = \frac{\omega}{v}\left(1+\frac{i}{2Q}\right)\sqrt{1-X^2} - \frac{\omega}{v_0}\left(1+\frac{i}{2Q_0}\right)\sqrt{1-X_0^2} \qquad (6)$$

Where

$$X = \frac{s_x}{\left(1+\frac{i}{2Q}\right)}, \quad X_0 = \frac{s_{x0}}{\left(1+\frac{i}{2Q_0}\right)} = \frac{m_Q}{m}X, \qquad (7)$$

$$m = \frac{v(Q,\omega)}{v_0(Q_0,\omega)}, \quad \text{and} \quad m_Q = \frac{1+\frac{i}{2Q}}{1+\frac{i}{2Q_0}},$$

The square roots in equation 6 can be approximated as

$$R \equiv \sqrt{1-X^2} \approx 1 - \frac{aX^2}{1-bX^2},$$

Combining the fractions into one, and keeping only the first-order terms, the operator $s_{zQ}$, can then be approximated as:

$$s_{zQ} = m\sqrt{\left(1+\frac{i}{2Q_0}\right)^2 - \frac{s_x^2}{m^2}} + (1-m) + \frac{i}{2}\left(\frac{1}{Q}-\frac{m}{Q_0}\right) - \left(1+\frac{i}{2Q}\right)\frac{a\left(1-\frac{m_Q}{m}\right)s_x^2}{\left(1+\frac{i}{2Q}\right)^2 - b\left(1+\frac{m_Q^2}{m^2}\right)s_x^2}. \qquad (8)$$

The combination of the first three terms of equation (8) is a split-step Fourier like operator while the fourth term is a Finite-Difference operator that can be implemented as an implicit scheme.

Similarly to the non-attenuating case, equation (8) can be adapted to account for TTI anisotropy by using odd and even rational function terms in the finite differences (Valenciano et al., 2009).

**Synthetic data example**

Using viscoacoustic ray tracing we generated two datasets based on a constant velocity model that includes 7 flat reflectors. The first dataset was generated assuming an acoustic medium while attenuation effects were included in the second dataset using the Q model shown in Figure 1.

Figure 2 shows the frequency spectrum of the bottom reflector from both datasets. Notice the decay in amplitudes and frequency content of the bottom reflector in the attenuating medium. The amplitude spectra after migration are shown in Figure 2 while Figure 3 compares the migration images with and without attenuation compensation. Both figures demonstrate that the migration with attenuation compensation successfully recovers the phase and amplitude spectra.

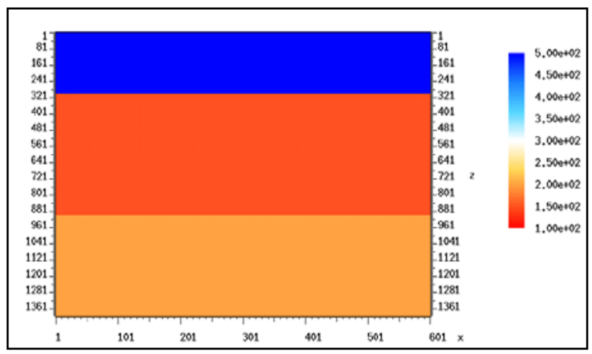


Figure 1: Q model for the flat reflector data.

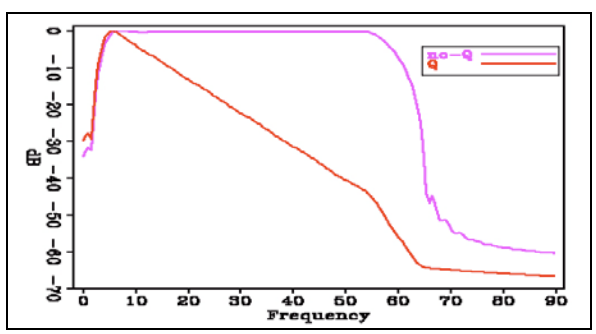


Figure 2: Power spectra of the bottom reflector in the synthetic model

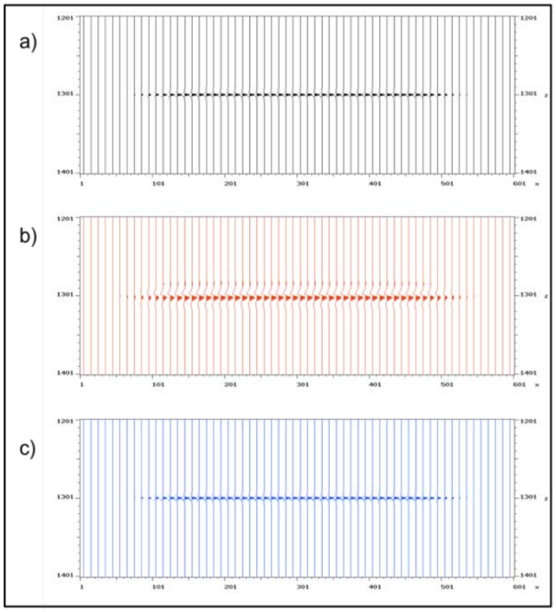


Figure 3: Migration results: a) No Q effects in modeling and migration, b) data modeled with Q effects and migrated without Q compensation, and c) data with attenuation effects and migration with Q compensation.

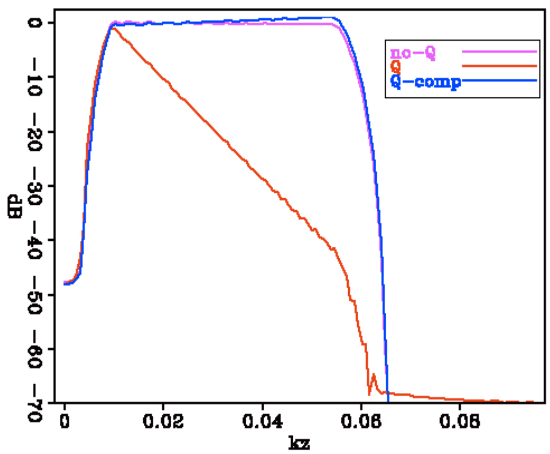


Figure 4: Wavenumber spectra for the bottom reflector from different migrations.

## Field data example from North Sea

We applied the migration with Q compensation to a 3D dataset from the North Sea acquired with dual-sensor streamers comprised of hydrophones and vertical geophones. Dual-sensor wavefield separation was applied to the data to produce upgoing and downgoing pressure wavefields at the sea surface (z=0). By using spectral ratios techniques we derived the depth Q model (Figure 5).

Figures 6a and 6b show a comparison of the migration without (Figure 6a), and with Q compensation (Figure 6b). The image resolution is largely improved by successfully recovering the high wavenumber components after migration with Q compensation.

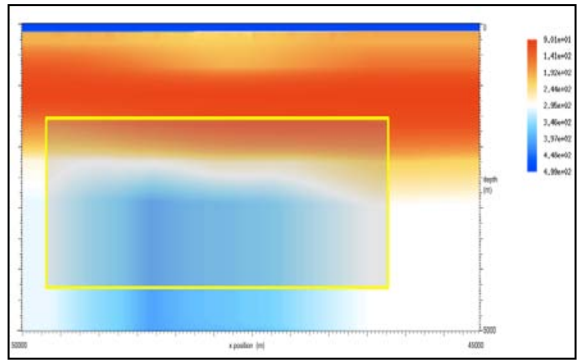

Figure 5: Q model for the North Sea dataset

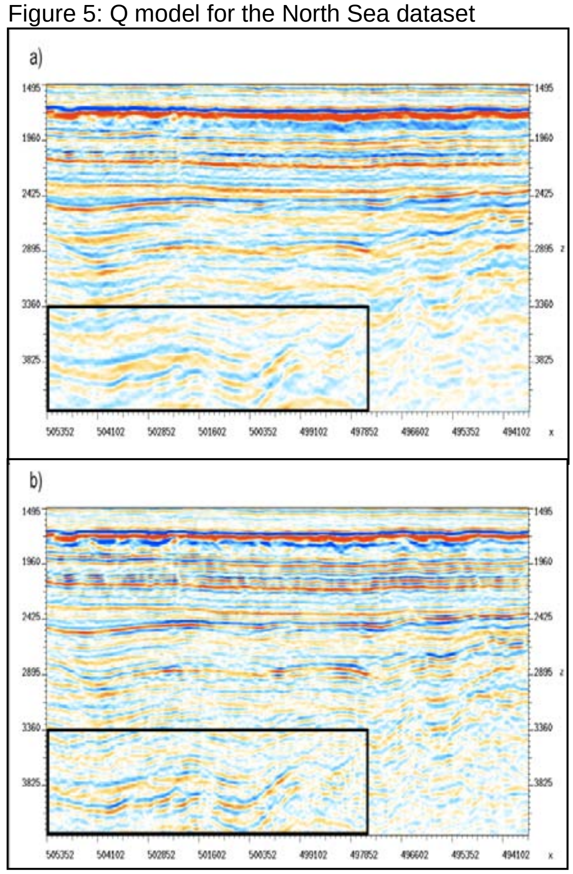


Figure 6: Migration of the North Sea data: a) without Q compensation, b) with Q compensation.

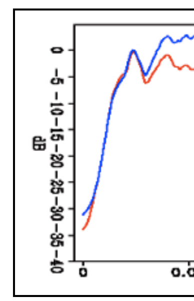

Figure 7: Power Spectrum of the North Sea images, red without Q compensation, and blue with Q compensation

## Field data example from Gulf of Mexico

We also applied the migration with Q compensation to a dataset from deep water Gulf of Mexico. The data were acquired using dual-sensor streamer recording. The area (Desoto Canyon) is characterized by vertical transverse isotropy. Therfore, the migration needed to account for the attenuation as well as the VTI properties of the earth model. Our PSDM jointly incorporated both effects in a single solution.

Figures 8 and 9 show a comparison of the migration without (Figure 8), and with Q compensation (Figure 9). The image resolution is largely improved by incorporating attenuation in the migration. This is also demonstrated in Figure 10 that shows broader wavenumber spectrum after Q compensation.

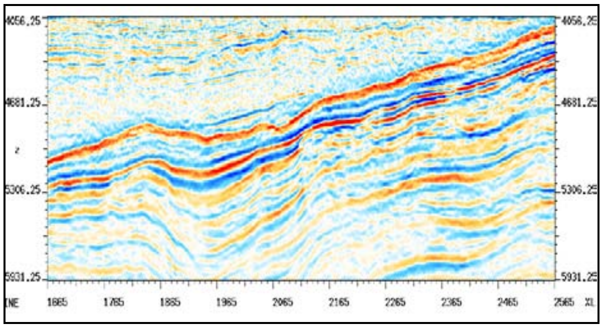


Figure 8 Migration without Q compensation of the VTI GOM dataset

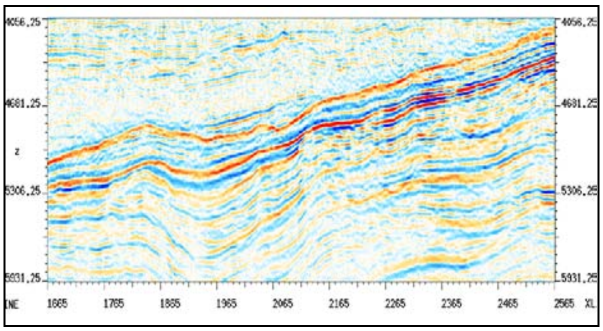


Figure 9: Migration with attenuation compensation of the VTI GOM dataset

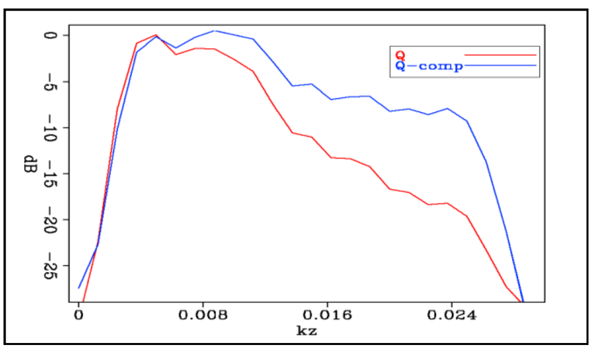


Figure 10: Power spectrum of the Gulf of Mexico images. Red is the wavenumber spectrum from WEM without Q compensation; Blue is the spectrum from WEM with Q compensation.

## Conclusions

We present a Fourier Finite-Difference (FFD) solution for viscoacoustic migration by wavefield continuation. The approximation of the dispersion relation with attenuation can be built using a Padé's rational series expansion in the wavenumber domain, which translates to implicit finite-differences schemes in the space domain. Unlike the non-attenuating case, the Padé's expansion in presence of attenuation has an imaginary part that recovers the high vertical wavenumbers; therefore improving resolution and amplitude balancing of seismic images.

In presence of anisotropy, the proposed PSDM can jointly incorporate attenuation and anisotropic effects in a single solution. Moreover the algorithm naturally reduces to the isotropic acoustic case in absence of attenuation and/or anisotropy.

Significant improvements in image quality can be achieved by incorporating attenuation in the migration. This is demonstrated by the migration of a synthetic dataset, and two dual-sensor towed streamer surveys from the North Sea and the Gulf of Mexico.

## Acknowledgments

We thank PGS for the permission to publish this work.

## References

- Causse, E., and Ursin, B., 2000, Viscoacoustic reverse-time migration: Journal of Seismic Exploration, **9**, 165-184.
- Chen Y., and Huang Y., 2010, Use Q-RTM to Image Beneath Gas Hydrates in Alaminos Canyon, Gulf of Mexico: SEG Expanded Abstracts 29, 3165-3170.
- Dai N., and West G. F., 1994, Inverse Q migration: SEG Expanded Abstracts 13, 1418-1421.
- Futterman, W. I., 1962, Dispersive body waves: J. Geophys. Res., **67**, 5279-5291.
- Mittet R., Sollie R., and Hokstad K., 1995, Prestack depth migration with compensation for absorption and dispersion: Geophysics, **60**, 1485.
- Ristow D., and T. Ruhl, 1994, Fourier finite-difference migration: Geophysics, **59**, 1882.
- Robinson, J., A technique for the continuous representation of dispersion in seismic data: Geophysics, **44**, 1345.
- Valenciano, A. A., C. C. Cheng, N. Chemingui, and S. Brandsberg-Dahl, 2009, Fourier finite-difference migration for 3D TTImedia: 71st EAGE Conference & Exhibition, P065.
- Wang Y., 2008, Inverse-Q filtered migration: Geophysics, **73**, 1.
- Yu Y., Lu R. S., and Deal M. M., 2002, Compensation for the effects of shallow gas attenuation with viscoacoustic wave-equation migration: SEG Expanded Abstracts 21, 2062-2065.
- Zhang Y., Zhang P., and Zhang H., 2010, Compensating for visco-acoustic effects in reverse-time migration: SEG Expanded Abstracts 29, 3160-3164.